HAMMOCK EFFECT CONTRIBUTION TO BEARING CAPACITY IMPROVEMENT OF GEOCELL REINFORCED SOIL

Bobby Prayogo CHANDRA[1], Takashi KIYOTA[2], Michiyuki HARATA[3], Masataka SHIGA[4], Matthew CHUA[5], and Toshihiko KATAGIRI[6]

ABSTRACT:

Constructing on weak soil could no longer be avoided as the land area is limited. To turn the weak soil to meet the standard of bearing capacity and settlements, researchers and engineers has developed various methods such as the use of geocell as soil reinforcement technique. Geocells are 3-dimensional interconnected cells made up of high tensile strength polymers. The objective on this study is to have a further understanding of one of geocell mechanism, the hammock effect, as there was no standardized procedure yet for designing a geocell reinforced system. To achieve the objective, laboratory test was conducted using a honeycomb-shape hand-made geocell made of plastic grid mesh-like material by varying the width, assisted with digital image correlation (DIC) analysis.

Key Words: *Geocell, Bearing Capacity, Settlement, Hammock Effect, Digital Image Correlation (DIC)*

INTRODUCTION

In this era of rapid urbanization is followed by the increasing demand in land use for housing and infrastructure, where it is inevitable to constructing structures in an originally unqualified area. Most common problem of these soils are primarily the insufficient bearing capacity and excessive deformation. Researchers and engineers have developed methods to improves the strength and stiffness of the soil and reduce soil's susceptibility to compression and liquefaction (Biswas & Krishna, 2017). Numerous techniques to improve the settlement-bearing capacity of soil includes soil stabilization and soil reinforcement in which by inclusion of reinforcement is a reliable technique to improve the soil properties (Zhou & Wen, 2007). Earth reinforcement that are widely used to improve soil behavior are geosynthetics (Kargar & Hosseini, 2016) as they can perform well and improves the safety factor (Marto et al., 2013) while being economical and simple on field application.

Geocell is one of the geosynthetic ground reinforcement which is three-dimensional in shape and made up of high tensile strength polymers welded together. The three-dimensional shape enables geocell to encapsulate the soil and thus, confined the soil and increase the soil bed performance (Hedge, 2017). There are three reinforcement mechanism of geocell-reinforced layer which is: (1) confinement effect: the mechanism works by confining the soil within the cell, arresting the lateral movement and increases

[1] Graduate Student, Dept. of Civil Eng. The University of Tokyo
[2] Associate Professor, Institute of Industrial Science, The University of Tokyo
[3] Plastic Products, Technical & Engineering Tokyo Printing INK MFG. Co., Ltd.
[4] Assistant Professor, Institute of Industrial Science, The University of Tokyo
[5] Doctoral Student, Dept. of Civil Eng. The University of Tokyo
[6] Senior Technical Specialist, Institute of Industrial Science, The University of Tokyo

the shear strength of filled materials and frictional resistance of the interface between the filled soil and cell wall, (2) vertical stress dispersion effect: the mechanism works by distributing the pressure over a wider area, resulting in a lower pressure exerted to the soft subgrade, and (3) hammock effect works by using the tension strength of the geocell material to produce the resisting upward force as the soil structure deforms vertically and bends the geocell (Zhang et al., 2009).

The purpose of this study is to get a better understanding of the aforementioned mechanisms, particularly the hammock effect, by observing the changes in stress-deformation behavior as the width of the geocells were varied. As there are still no standardize design procedure of geocell-reinforced soil design (Zhang et al., 2009), the outcome of this study could be one of the cornerstones for the development of better design procedures.

MATERIAL, TEST APPARATUS, AND PROCEDURE

Soil Box, Loading Apparatus and Footing

The main components of the test setup comprise of the soil box, the loading system and the measuring system. The loading system used was a modified strain-controlled machine developed in the Institute of Industrial Science of the University of Tokyo.

All the experiments were conducted inside a soil box container made of aluminum with an acrylic front panel so that the experiments could be observed. The volumetric dimension of the soil box is 140 mm in length, 670 mm in width and 580 mm in height.

The footing used is made of aluminum with the dimension of 135 mm in length, 50 mm width and 25 mm in height. The bottom face of the footing was attached with sandpaper to increase the surface roughness in order to avoid slippage between the interface of the footing and the underlying soil.

Figure 1 shows the experimental arrangement.

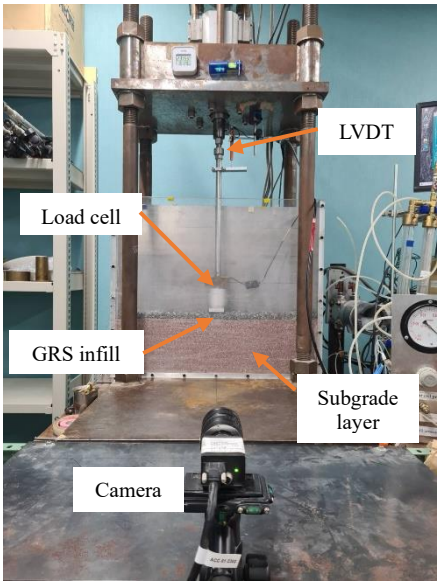

Figure 1. Test arrangement

Geocell model

The geocell model used in these tests were made of plastic grid mesh-like material that are commonly used in gardening. The thickness of each grid line is approximately 1 mm, with the spacing between them approximately 25 mm. The plastic mesh was then cut into a long strip and connected with a metallic pin to create the geocell into a honeycomb shape. Commercially available geocell has the cell dimension of 210 mm x 250 mm, creating a ratio of 0.84 and cell depth of 150 mm (Hedge & Sitharam, 2015). While in this study the size of each cell has an approximate ratio of 0.8 with the approximate size of 24.5 mm x 30 mm and height of 15 mm. Figure 2 and Figure 3 show the schematic dimension of the cell size used and an example of the geocell model respectively. The plastic grid strip has the young modulus of 1032 MPa.

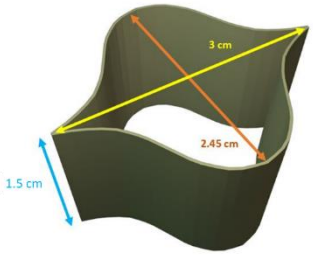

Figure 2. Cell dimension illustration

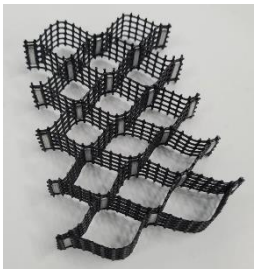

Figure 3. Geocell model

Backfill material

Two types of backfill material were used, Silica sand no. 5 for the subgrade material and gravel no. 1 for the geocell reinforced bed infill layer. The physical and mechanical properties of both materials are shown below on table 1 The particle size distribution is shown in Figure 4.

For the purpose of digital image correlation analysis, the silica sand no. 5 used are a mixture of dyed and undyed one's with the ratio of 50:50 because distinct speckle patterns are essential.

Table 1. Properties of silica sand no. 5 and gravel no. 1

Property	Silica sand no. 5		Gravel no. 1	
	Value	Units	Value	Units
Specific gravity (G_s)	2.645		2.754	
Optimum moisture content	17.34	%	1.54	%
Minimum density	1.31	g/cm^3	1.75	g/cm^3
Maximum density	1.53	g/cm^3	1.91	g/cm^3
D_{50}	0.573	mm	3.314	mm
D_{10}	0.345	mm	2.328	mm
D_{30}	0.484	mm	2.903	mm
D_{60}	0.625	mm	3.48	mm
Coeff. of Uniformity (C_u)	1.81		1.49	
Coeff. of Curvature (C_c)	1.09		1.04	

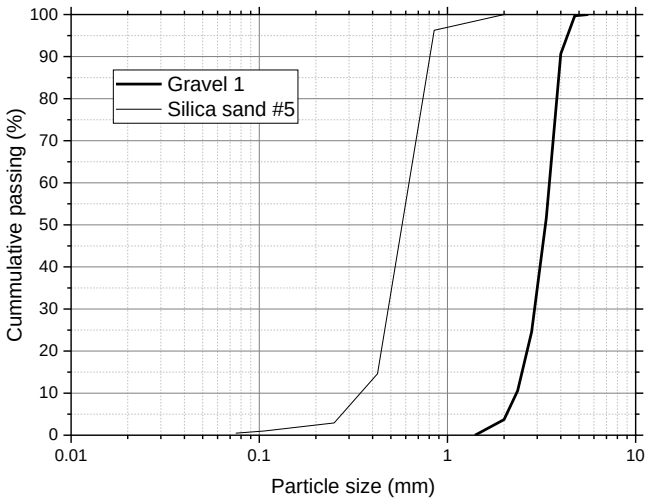

Figure 4. Particle size distribution of silica sand no. 5 and gravel no. 1

Experiment methodology

Silica sand no. 5 was first filled into the soil box as the subgrade layer and then followed by the placement of geocell with gravel no. 1 as the infill layer on top of the sand. The Silica sand no. 5 was poured in 9 different pouring stages with each stage filled the soil box for 20 mm thick until it reaches the expected depth of 180 mm with the Dr of 50%. Then, geocell model that was filled with gravel no. 1 with the Dr of 50-60% was place on top of the sand at the center, followed by the backfilling with gravel no. 1 to bury the geocell reinforced model with the DR of 10% until the gravel layer has the thickness of 25 mm and reach the expected height of 205 mm. To achieve the target DR, both the sand and gravel was poured at zero drop height for each sub layer to have relatively even compaction. Finally, the footing model was place on top of the soil at the center of the soil box.

However, compaction of the geocell infill material could not be done inside the soil box as compacting directly on top of the sand will disturbed and cause uneven distribution of the relative density. The technique used in this study to achieve the desired DR was by creating a mold, place the geocell and the infill material inside the mold and compact the infill in the mold. Figure 5 shows an image of the mold and compacted geocell reinforced bed. To move the geocell and the compacted infill material, the whole geocell reinforced bed was frozen and then removed from the mold to be place inside the soil box. Before every test, the geocell reinforced bed was let to thawed.

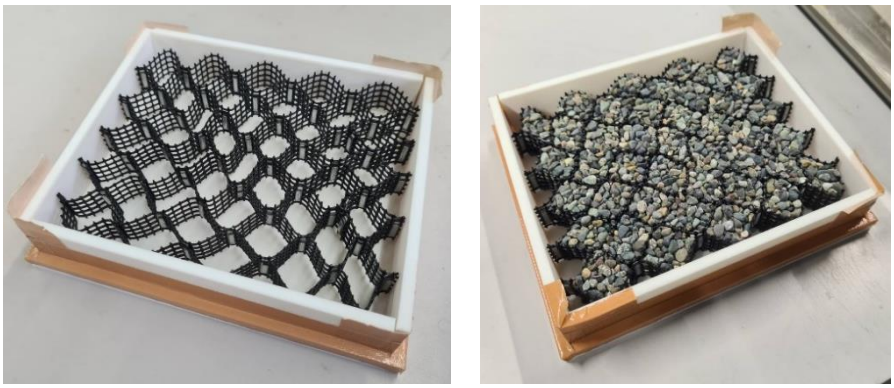

Figure 5. Mold and geocell model before and after filled with compacted gravel no. 1

Building a full setup of instruments to measure deformation can be expensive and yet the data acquired are limited to a specific location and discrete (Munoz & Kiyota, 2019). Other method that can be utilized to obtain deformation, displacement and motion of an object is by capturing digital images and performs image analysis. This non-contact measurement method called as digital image correlation (DIC) (Sutton et al., 2009). DIC works by comparing the changes of grey intensity of the captured images from the initial stage with the subsequent images of each loading stages through mathematical correlations. Unlike contact method that uses conventional measuring instruments such as pressure sensors and strain gauges, DIC does not affect the soil properties and no indeterminate variables to be concern such as the accuracy of sensors (Gedela et al., 2021).

To obtain a record of images for the digital image correlation (DIC) analysis, one last setup that needs to be prepared was the high-speed capturing camera on top of an adjustable stand. The camera was placed perpendicular to the acrylic facing of the soil box. The image taken includes the position of geocell placement before being buried by the infill material (gravel no. 1) and the geocell final position and shape after the test by excavating the soil on the opposite side of the acrylic facing.

The test cases that were done was to compare the effect of varying the geocell width to an approximate value of once (1B), twice (2B) and three times (3B) the footing width (B).

Table 2. Experiment cases

No.	Cases	Geocell			Infill Dr (%)
		Height (mm)	Length (mm)	Width (mm)	
1	Unreinforced	-	-	-	-
2	1B	15	122.5	60	46.78
3	2B	15	122.5	90	57.32
4	3B	15	122.5	145	54.23

*B is the width of the footing model which is 50 mm

TEST RESULTS AND DISCUSSIONS

Effect of geocell width on bearing capacity

The test results indicates that the bearing capacity improves as the geocell width increases until 3B, three times the width of the footing. However, the improvement by increasing the width from 2B to 3B was not as significant as comparing from unreinforced to 1B or 1B to 2B as shown in Figure 6.

It seems that the geocell reinforcement did not provide its full contribution until the S/B exceeds above 0.6. However, that does not mean that the geocell reinforcement does not contribute to the soil strength at the early stage. The results indicate that all the reinforced cases have a slightly higher initial stiffness compared to unreinforced condition at S/B lower than 0.6 with the case 3B having the highest stiffness. At S/B higher than 0.6, the geocell reinforced cases show a sudden increase in stiffness, especially for case 3B where it has the highest stiffness while the case 1B and 2B has the same stiffness. Not until it reached the S/B of 0.12 that the case 2B became stiffer than 1B. Nevertheless, the geocell reinforced system seems only able to maintain the high stiffness value until the S/B reached over 0.2. For case 2B and 3B, the reinforced soil stiffness still increasing at a slower rate with at which the increment for both cases appears as if they are the same. For case 1B, the increase is less significant and starts to plateau.

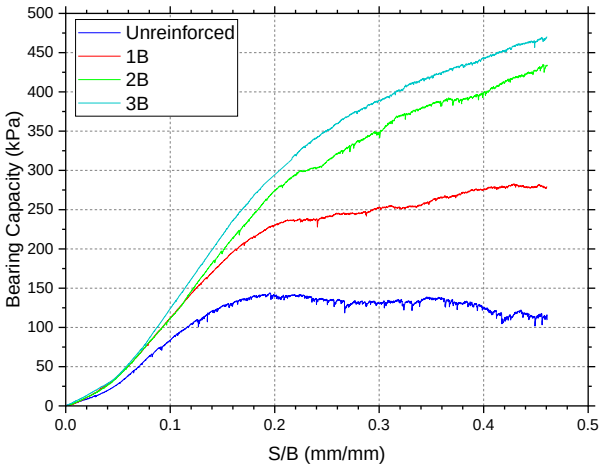

Figure 6. Bearing capacity – displacement curves

Hammock effect mechanism

Zhang et al. (2010) proposed a method to calculate the improvement contribution of the stress dispersion effect and hammock effect mechanism with the following formula.

$$\Delta p_1 = \frac{2h_c tan\theta_c}{b_n} p_s$$

$$\Delta p_2 = \frac{2Tsin\alpha}{b_n}$$

Where Δp_1 is bearing capacity increment due to stress dispersion effect, Δp_2 is bearing capacity increment due to hammock effect, h_c is the thickness of geocell reinforcement, θ_c is the angle of dispersion of geocell reinforcement, b_n is the width of the footing, p_s is the bearing capacity of unreinforced soil, T is the tensile force of the geocell reinforcement and α is the horizontal angle of the tension force.

With the help of image analysis and digital image correlation (DIC), the tensile force T and horizontal angle of the tension force α could be calculated and the dispersion angle θ_c could be acquired.

(1) 60 mm width geocell (1B)

Figure 7 shows the image before and after the test 1B, about the position and shape of the geocell and the soil profile. By superimposing the images, the geocell and soil profile could be traced. Figure 8 shows that the geocell does not change in shape before and after the test but instead only change in position due to settlement. Also, the shape of the geocell does not in-line with the soil profile after the test as shown in Figure 9.

By breaking down the particle movement obtain from the digital image correlation analysis results into the y-component, the images showing obvious dispersion angle as shown in Figure 10 at S/B = 0.46. Based on the proposed calculation method by Zhang et al. (2010), the contribution of the geocell to the bearing capacity increment could be calculated. The measured dispersion angle of different S/B were listed on table 3. Since the geocell shape remain the same, there are no hammock effect taking place. The calculated and experimental result seems to have a good correlation at smaller displacement until S/B = 0.15 where after that the calculation method is no longer applicable (see Figure 11).

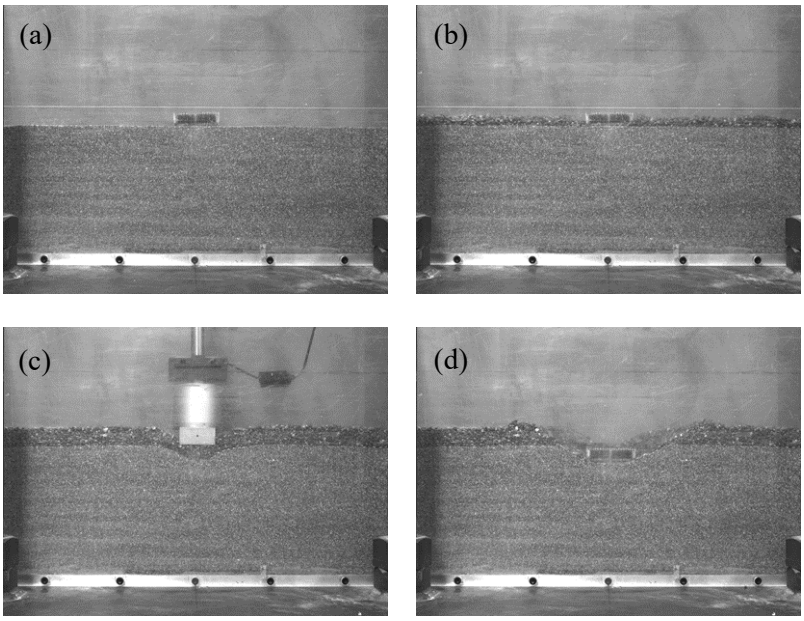

Figure 7. Case 1B (a) Frozen geocell reinforced bed, (b) Thawed geocell reinforced bed, (c) Soil profile after the test (unexcavated), (d) Geocell position and shape after the test (excavated)

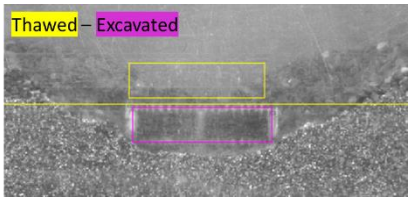

Figure 8. Traces of superimposed images between thawed and excavated state of 1B

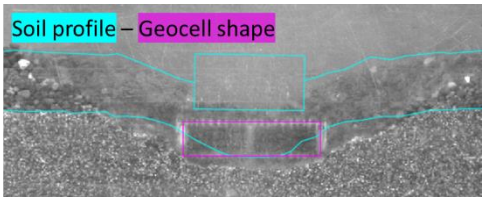

Figure 9. Traces of superimposed images between soil profile and geocell shape after the test of 1B

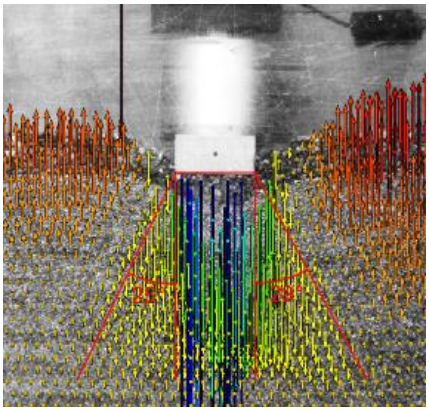

Figure 10. Dispersion angle at S/B = 0.46 of case 1B

Table 3. Dispersion angle of case 1B

Disp. (mm)	S/B	θc (˚)
4.0	0.08	25.5
5.0	0.10	25.5
7.5	0.15	26.5
10.0	0.20	27.0
15.0	0.30	25.0
20.0	0.40	26.5
23.0	0.46	26.5

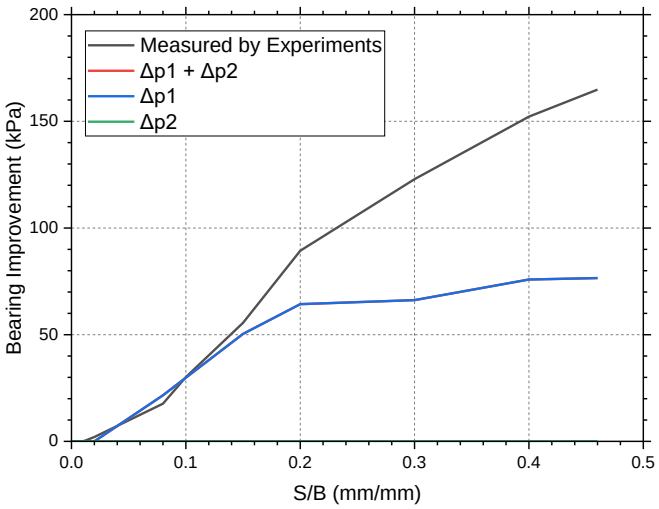

Figure 11. Bearing capacity improvement of case 1B

(2) 90 mm width geocell (2B)

With the same method as the 1B case, contribution of the geocell to the bearing capacity increment could be calculated. However, in case 2B, as Figure 13 shown that the geocell was bended but settled at the same time. If the assumption that there is no settlement occurred, the calculated contribution of hammock effect at the end of the test was so minimal (see Figure 16) that it is safe to assume that the hammock effect does not contribute to every settlement stage for case 2B too. Table 4 provides the measured distribution angle and the calculated tension force and the horizontal angle of the tension force at different stages of S/B. The calculated bearing contribution of geocell correlates well until S/B = 0.15.

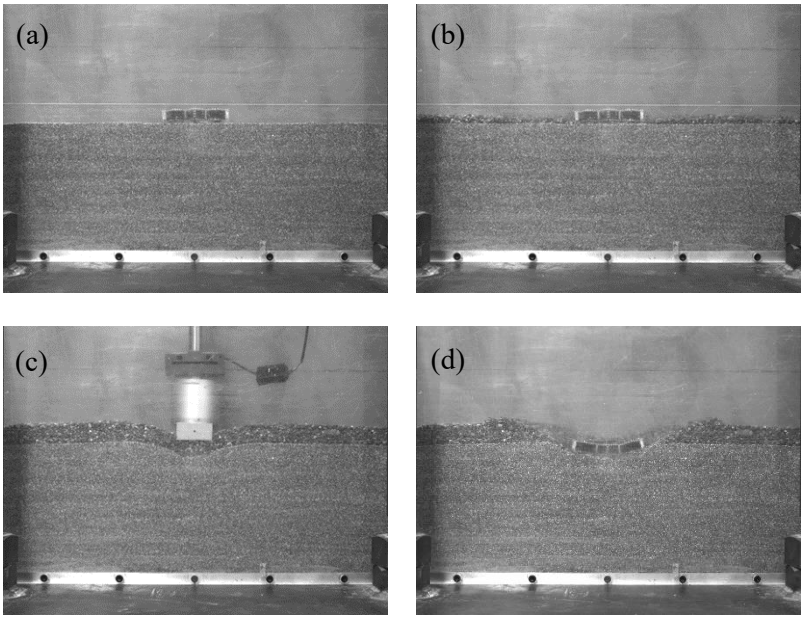

Figure 12. Case 2B (a) Freeze geocell reinforced bed, (b) Thawed geocell reinforced bed, (c) Soil profile after the test (unexcavated), (d) Geocell position and shape after the test (excavated)

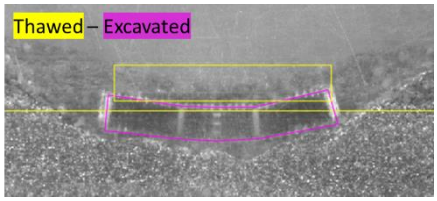

Figure 13. Traces of superimposed images between thawed and excavated state of 2B

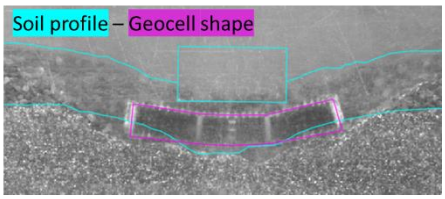

Figure 14. Traces of superimposed images between soil profile and geocell shape after the test of 2B

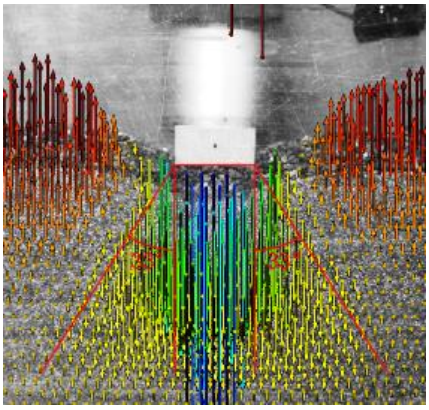

Figure 15. Dispersion angle at S/B = 0.46 of case 2B

Table 4. Dispersion angle, tension force and horizontal angle of tension force of case 2B

Disp. (mm)	S/B	θc (°)	T (N)	α (°)
4.0	0.08	26.5	-	-
5.0	0.10	27.5	-	-
7.5	0.15	27.5	-	-
10.0	0.20	29.0	-	-
15.0	0.30	30.0	-	-
20.0	0.40	33.5	-	-
23.0	0.46	33.0	95.47	9.72

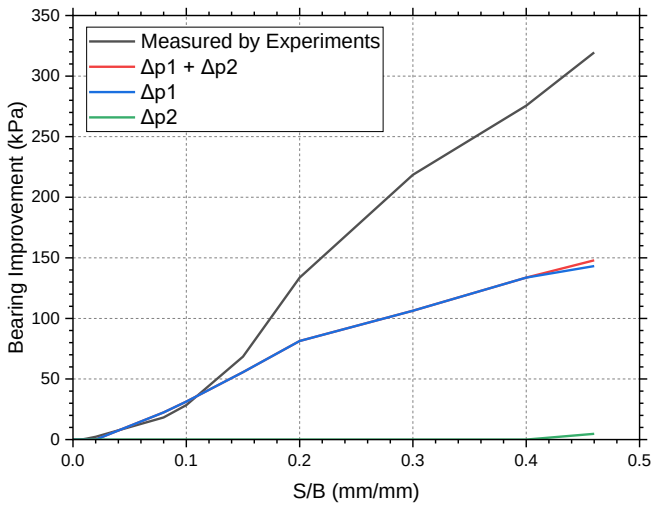

Figure 16. Bearing capacity improvement of case 2B

(3) 145 mm width geocell (3B)

Similarly, with the same method as case 1B and 2B was used for case 3B. But in case 3B the shape of the geocell corresponds quite well with the soil profile after the test as shown in Figure 18. Table 5 shows the measured distribution angle and the calculated tension force and the horizontal angle of the tension force.

For this case, the hammock effect contributes less at smaller displacement but gradually increases after the settlement exceed S/B = 0.1. The calculated total geocell contribution have a good correlation with the measured value from the experiment results.

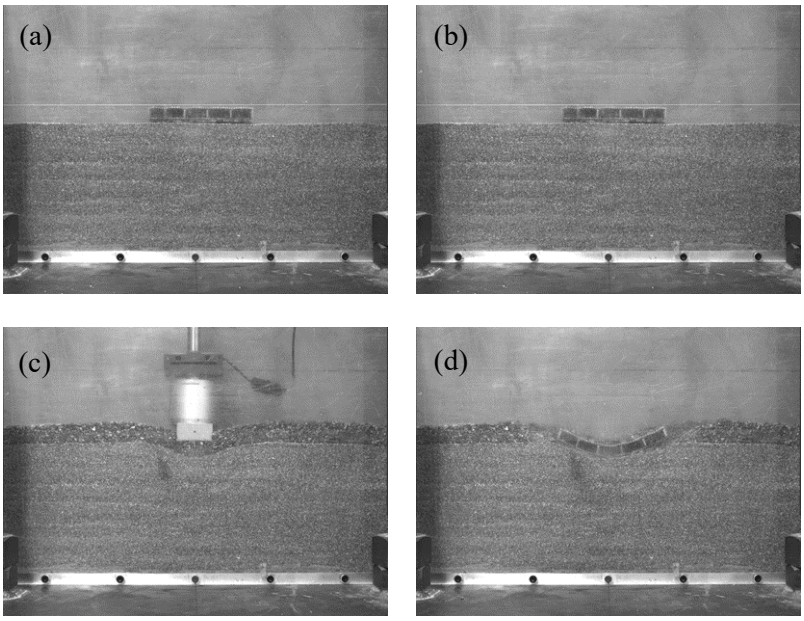

Figure 17. Case 3B (a) Freeze geocell reinforced bed, (b) Thawed geocell reinforced bed, (c) Soil profile after the test (unexcavated), (d) Geocell position and shape after the test (excavated)

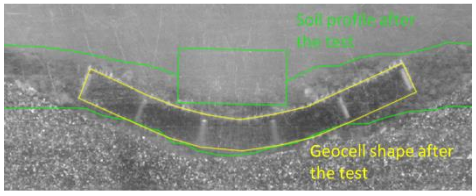

Figure 18. Traces of superimposed images between thawed and unexcavated state of 3B

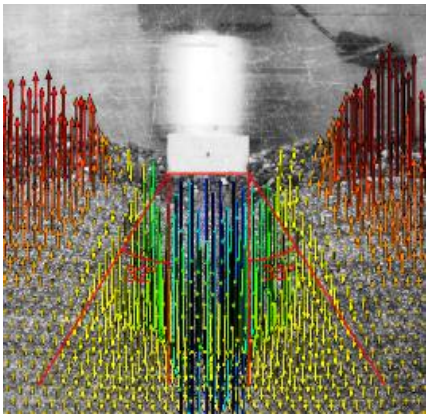

Figure 19. Dispersion angle at S/B = 0.46 of case 3B

Table 5. Dispersion angle, tension force and horizontal angle of tension force of case 3B

Disp. (mm)	S/B	θc (°)	T (N)	α (°)
4.0	0.08	26.0	147.26	12.02
5.0	0.10	27.5	164.04	12.67
7.5	0.15	29.0	259.48	15.82
10.0	0.20	31.0	348.25	18.21
15.0	0.30	31.5	628.65	23.98
20.0	0.40	32.5	877.90	27.86
23.0	0.46	32.5	1122.85	31.00

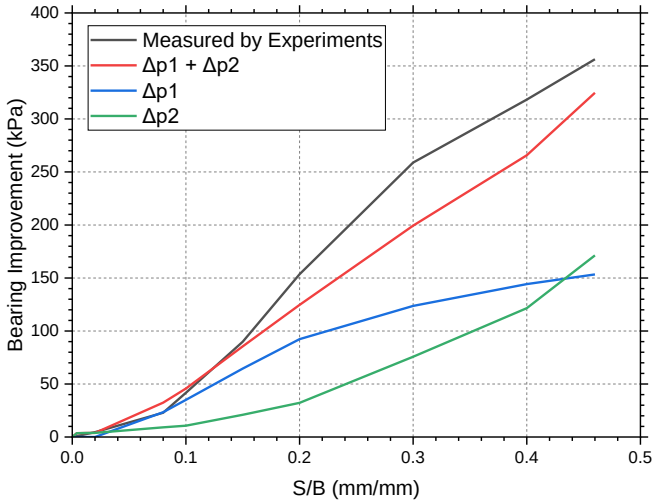

Figure 20. Bearing capacity improvement of case 3B

CONCLUSIONS

Results from the experiments concluded that the bearing capacity of reinforced soil by geocell increases as the width increases and this result was in-line with the result from previous researchers.

From the calculation result, all the different width cases have a good bearing improvement correlation with the measured value only at low settlement at S/B = 0.15. With the exception for the case 3B, the hammock effect contribution resulting the calculated total bearing improvement to have a good correlation with the measured value even on large settlement (S/B > 0.15). The similarities of all geocell width are that the calculated stress dispersion effect contribution starts to plateau after S/B larger than 0.15.

From the digital image correlation (DIC), the general trend found of the stress distribution is that the stress distribution angle θ_c gradually increases until it reaches a certain maximum angle. An interesting finding is that the dispersion angle of smaller geocell width (case 1B) is smaller than that of the wider geocell (case 2B and 3B) but almost the same dispersion angle was observed for case 2B and 3B.

Based on this finding, the hammock effect does not mobilize if the geocell reinforced bed was not wide enough for the geocell to mobilize anchoring mechanism. For the geocell to mobilize the hammock effect, it is best to use the width of at least three times the width of the footing.

REFERENCES

Biswas, A., & Krishna, A. M. (2017). Geocell-Reinforced Foundation Systems: A Critical Review. *Int. J. of Geosynth. and Ground Eng., 3,* Article 17. doi:DOI 10.1007/s40891-017-0093-7

Gedela, R., Kalla, S., Sudarsanan, N., & Karpurapu, R. (2021). Assessment of load distribution mechanism in geocell reinforced foundation beds using Digital Imaging Correlation Techniques. *Transportation Geotechnics, 31*. doi:https://doi.org/10.1016/j.trgeo.2021.100664

Hedge, A. (2017). Geocell reinforced foundation beds-past findings, present trends and future prospects: A state-of-the-art review. *Construction and Building Materials, 154*, 658-674.

Hedge, A. M., & Sitharam, T. (2015). Effect of infill materials on the performance of geocell reinforced soft clay beds. *Geomechanics and Geoengineering, 10*(3), 163-173. doi:10.1080/17486025.2014.921334

Kargar, M., & Hosseini, S. M. (2016). Influence of reinforcement stiffness and strength on load-settlement response of geocell-reinforced san bases. *European Journal of Environmental and Civil Engineering, 22*(5), 596-613. doi:10.1080/19648189.2016.1214181

Marto, A., Oghabi, M., & Eisazadeh, A. (2013). Effect of Geocell Reinforcement in Sand and Its Effect on the Bearing Capacity with Experimental Test; A Review. *Electronic Journal of Geotechnical Engineering, 18*, 3501-3516.

Munoz, H., & Kiyota, T. (2019). Deformation and localisation behaviours of reinforced gravelly backfill using shaking table tests. *Journal of Rock Mechanics and Geotechnical Engineering, 12*, 102-111.

Sutton, M. A., Orteu, J.-J., & Schreier, H. W. (2009). *Image Correlation for Shape, Motion and Deformation Measurements: Basic Concepts, Theory and Applications.* Springer.

Zhang, L., Zhao, M., Shi, C., & Zhao, H. (2009). Bearing capacity of geocell reinforcement in embankment engineering. *Geotextiles and Geomembranes, 28*, 475-482.

Zhou, H., & Wen, X. (2007). Model studies on geogrid- or geocell-reinforced san cushion on soft soil. *Geitextiles and Geomembranes, 26*, 231-238. doi:10.1016/j.geotexmem.2007.10.002